FILMWISE CONDENSATION ON MICRO-FIN SURFACES PRODUCED BY SELECTIVE LASER MELTING

Ho J.Y. * and Leong K.C.
*Author for correspondence
Singapore Centre for 3D Printing
School of Mechanical and Aerospace Engineering
Nanyang Technological University
50 *Nanyang Avenue*
Singapore 639798
Republic of Singapore
E-mail: jyho@ntu.edu.sg

ABSTRACT

This paper presents an experimental investigation on the condensation of steam on vertical flat surfaces with arrays of micro-fins. Three micro-fin surfaces (*MF*1, *MF*2 and *MF*3) of the same fin diameter and fin height but with different fin pitch were fabricated by selective laser melting. The surfaces were tested in a condensation chamber where the gravity driven condensate flow and vapor velocity are orthogonal to one another. The effects of fin pitch and vapor velocity on the heat transfer performances of the surfaces were examined. Our results suggest that fin pitch has significant influence on the condensate drainage path as compared to the increase in heat transfer area. In addition, above a certain wall subcooled temperature, the increase in vapor velocity also resulted in the systematic increase in condensation heat flux indicating the significant effects of vapor shear force. In all, up to 1.4 times enhancement in the heat transfer coefficient was achieved with the micro-fin surface with a fin pitch of 300 μm as compared to a plain Al-6061 surface at constant vapor velocity.

INTRODUCTION

Condensation heat transfer is used in many engineering systems such as desalination systems, condensers of power plants, air-conditioning systems and in the thermal management of electronic devices. Due to its ubiquitous applications, enhancing condensation heat transfer is of significant importance in improving system efficiency and reducing energy consumption. Even though dropwise condensation exhibits high heat transfer rates, filmwise condensation remains the dominant mode in many industrial applications [1]. Therefore, numerous research efforts have been placed on enhancing filmwise condensation and on the fundamental understanding of the intricate mechanisms involved.

The use of enhanced surface features such as integral and pin fins have been shown to enhance filmwise condensation. On top of the increased heat transfer area, effects due to gravity and surface tension forces also affect the heat transfer performances of these enhanced surfaces and have been considered in several models [2 - 5]. In addition, the condensate film characteristics were also shown to be affected by the fin geometries, dimensions and arrangements, which in turn influenced the heat transfer rate from the tip, flank and base of the fins.

NOMENCLATURE

A	[m^2]	Cross-sectional area
A_t	[mm^2]	Total heat transfer area
d	[μm]	Fin diameter
g	[m^2/s]	Gravitational acceleration
h	[$W/m^2 \cdot K$]	Heat transfer coefficient
h_{fg}	[J/kg]	Latent heat of vaporization
k_c	[W/m·K]	Thermal conductivity of copper
k_s	[W/m·K]	Thermal conductivity of specimen
l	[μm]	Fin height
p	[μm]	Fin pitch
q''	[W/m^2]	Heat flux
T	[ºC]	Temperature
U	[m/s]	Vapor velocity
Δy	[m]	Distance from T_s to T_w
μ	[kg/m·s]	Dynamic viscosity
ρ	[kg/m^3]	Density

Subscripts

l	Liquid
w	Wall
s	Saturation
v	Vapor
Nu	Nusselt
Mod	Modified

Honda et al. [6] studied the condensation performance of complex three-dimensional finned tubes and two-dimensional integral fins of different geometries and vapor velocities. It was determined that the flat-sided integral fin had the highest heat transfer performance. In addition, the increase in vapor velocity from 3.3 m/s to 18 m/s only increased the heat transfer coefficients of the tubes by up to 30%. Zhang et al. [7] investigated the condensation of R407C refrigerant with three-dimensional integral finned tubes with petal-shaped fin geometries (or PF tubes) where enhancement factor of 4.6 to

5.35 as compared to a smooth tube was recorded. A systematic study on the effects of vapor velocity on the condensate retention angle on integral fins was performed by Fitzgerald et al. [8] in a wind tunnel. For water as test fluid, it was determined that the condensate retention angle decreased with increasing air velocity. Subsequently, Ali and Abubaker [9] extended the studies to include pin fins of different circumferential thicknesses and observed that as the vapor velocity approached zero, the increase in circumferential fin thickness decreased the retention angle. On the other hand, at high vapor velocity, vapor shear was observed to have less influence on the retention angle.

Apart from fin geometry and vapor velocity, studies on effects of fin spacing on film condensation performance have also been carried out by previous researchers. The decrease in fin spacing results in the increase in fin density and area for heat transfer surface. However, condensate may also accumulate in between the the fins and adversely affect condensate drainage and heat transfer. Yau et al. [10] experimentally investigated integral finned tubes of different fin spacings (0.5 to 20 mm) with steam and determined that the fin spacing of 2 mm achieved the optimal heat transfer performance. Recently, the effect of circumferential spacing of pin fin (S_c) was reported by Ali and Briggs [11] in which the S_c values of 0.5 mm demonstrated the highest heat transfer enhancement ratio.

Based on the above brief review, it can be seen that gravitational and liquid-vapor interfacial shear forces are the main mechanisms affecting filmwise condensation and fin parameters such as fin geometry and spacing have direct influence on these mechanisms which in turn affect the condensate film thickness profile and condensate retention. However, existing works on external surface filmwise condensation were mainly focused on on-tube condensation with integral and pin-fins while investigations on the use of microstructures for enhancing filmwise condensation under the combined influence of vapor shear and gravitational forces are scarce. In this paper, filmwise condensation on micro-fin surfaces of different fin pitches is investigated where the vapor flow and gravity driven condensate flow are in orthogonal directions. Using the Selective Laser Melting (SLM) technique, highly-ordered micro-fin surfaces were produced and effects of fin pitch and vapor flow rate on the heat transfer performance were examined.

FABRICATION AND CHARACTERIZATION OF MICRO-FIN SURFACES

The micro-fin surfaces employed in the present investigation were fabricated using the SLM 250 HL (SLM Solutions GmbH) facility in the Singapore Centre for 3D Printing of Nanyang Technological University, Singapore. An aluminum alloy (AlSi10Mg) of 20 µm to 63 µm size distribution was used as the base powder. A Gaussian distributed Yb:YAG laser with a maximum power of 400 W and a laser beam spot size of 80 µm was utilized to melt and fuse the powder layer-by-layer based on the input of a Computer Aided Design (CAD) model. In the present investigation, a laser power of 350 W, scanning speed of 1150 mm/s and hatching spacing of 0.17 mm were selected. For each surface, the micro-fin array is fabricated onto a 25 mm × 25 mm × 5 mm base plate as an integrated build piece. All the micro-fin surfaces have the same fin diameter of 300 µm and fin height of 600 µm but with different fin pitches in order to explore the effects of fin spacing on the specimens' heat transfer performance. As a result of the difference in fin pitch, the total heat transfer area between each surface also differs. In the present investigation, three surfaces (*MF*1, *MF*2 and *MF*3) of different fin pitches were investigated. A photograph of the micro-fin surface (*MF*3) is depicted in Fig. 1 and a top view of the microscopic image of *MF*3 is shown in Fig. 2. The parameters of all the micro-fin surfaces are summarized in Table 1.

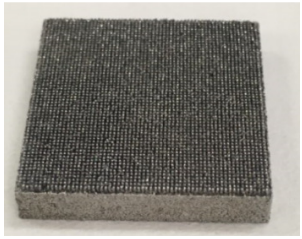

Figure 1 Image of Micro-fin surface (*MF*3).

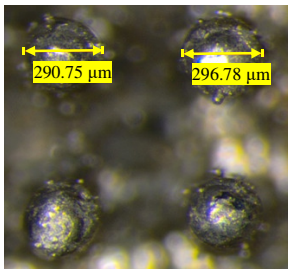

Figure 2 Top view of microscope image of micro-fin surface (*MF*2).

Table 1. Parameters of micro-fin surfaces investigated.

No.	Fin pitch, p (µm)	Total heat transfer area, A_t (mm^2)
*MF*1	900	978
*MF*2	600	1576
MF3	300	2729
All the micro-fin surfaces have the same fin diameter (d) and fin heights (l) of 300 µm and 600 µm, respectively.		

EXPERIMENTAL SETUP AND PROCEDURES

A schematic of the experiment setup which consists of a vapor loop and a water loop is shown in Fig. 3. A variable water speed pump was used to supply water to the evaporator which in turn generates steam to the condensation chamber. The vapor mass flow rate through the chamber was controlled by setting the water pump speed. The steam temperature can be adjusted by varying the evaporator heating power. As the mass flow rate of the water entering the evaporator is equal to the mass flow rate of steam leaving, the vapor velocity through the

condensation chamber can be determined from a rotameter that is positioned before the evaporator. Details of the condensation chamber are shown in Fig. 4. The specimen is fixed onto the top surface of the copper block. As the vapor comes into contact with the specimen, chilled water is allowed to circulate through the water channels at the base of the copper block to maintain the specimen top surface at subcooled temperature (T_w). Using the four thermocouples (T_1 to T_4) that are positioned along the copper block, each at 10 mm apart, the condensation heat flux (q'') can be determined using Eq. (1). Using the thermocouple embedded within the specimen, the temperature of the specimen (T_s) at 1.5 mm below the condensing surface was obtained and by Eq. (2), the temperature of the condensing surface (T_w) was computed. In Eqs. (1) and (2), k_c and k_s denote the thermal conductivities of copper and the aluminum alloy specimens, respectively whereas $\frac{dT}{dx}$ represents the temperature gradient between T_1 and T_4 and Δy represents the distance from T_s to T_w. Finally, using Eq. (3) the condensation heat transfer coefficient (h) can be calculated. The experiments were conducted at close to ambient pressure. In addition, the inlet vapor temperature was maintained at 1.0°C above the saturation value to ensure constant inlet vapor quality and the inlet chilled water supply was varied between at 40°C to 23°C. Finally, a gear pump was used to vary the chilled water flow rate through the copper block which in turn varied ΔT_s. A vacuum pump was first employed to remove any trace of non-condensable gas and thereafter vapor generated from the evaporated was used to flush the condensation chamber continuously for up to an hour prior to the start of the experiment. Using the method by Moffat [14], the uncertainties of q'' and h were determined to be ± 12.2% and ± 13.8%, respectively.

$$q'' = -k_c \frac{A_1}{A_2}\frac{dT}{dx} \tag{1}$$

$$T_w = T_s + \frac{q''\Delta y}{k_s} \tag{2}$$

$$h = \frac{q''}{T_w - T_s} = \frac{q''}{\Delta T_s} \tag{3}$$

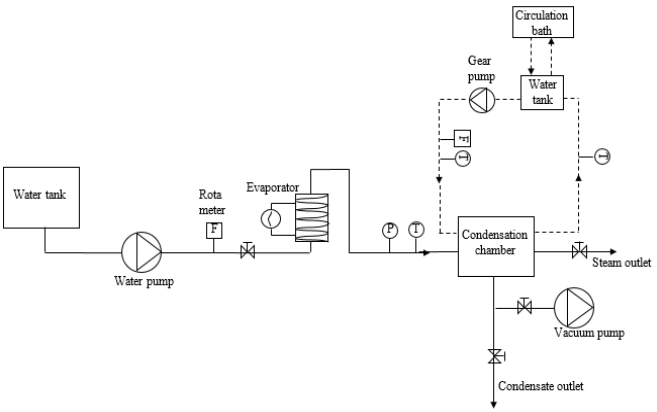

Figure 3 Schematic of experimental setup

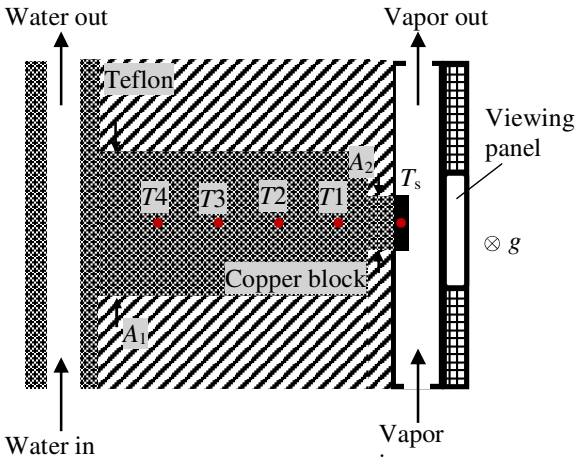

Figure 4 Top view of condensation chamber.

RESULTS AND DISCUSSION

A commercial Al-6061 surface which served as the control surface for comparison against the micro-fin structures was tested to validate the accuracy of the setup. Figure 5 shows typical temperatures recorded from thermocouples T_1 to T_4 along the copper block. It can be seen that the temperatures vary linearly with the axial direction (Δx) and, therefore, the 1-D heat conduction assumption used to compute the condensation heat flux as shown in Eq. (1) is valid.

A model for predicting filmwise condensation on a vertical plate was originally proposed by Nusselt [12], as shown in Eq. (4), in which the condensate flow was assumed to be driven by gravity and the surrounding vapor was assumed to be stagnant. During the condensation process, the formation of waves at the liquid film surface was observed by several researchers even when the flow was laminar and the surface was polished [1, 13]. To approximate the enhancement due to the effects of wave formation, a factor of 1.15 is typically multiplied to the Nusselt's model as shown in Eq. (5) [13], where h_{Mod} denotes the heat transfer coefficient predicted by the modified Nusselt's model. It should be noted that in Eq. (5), the effects of the condensate film inertia and vapour shear are neglected. In order to replicate the assumptions made in the above model, the Al-6061 surface was tested at low vapor velocity (U) of 0.72 m/s, which is close to 0 m/s. The experimental results of the plain Al-6061 surface and the computed q'' values using Eqs. (4) and (5) are shown in Figure 6. It can be seen that the experimental results lie closer to the modified Nusselt's model. In addition, the deviation between Eq. (5) and the experimental values is < 6.5%, which is lower than the experimental uncertainties.

$$h_{\mathrm{Nu}} = \frac{q''_{\mathrm{Nu}}}{\Delta T_s} = 0.943\left[\frac{\rho_l(\rho_l - \rho_v)g h_{fg} k_l^3}{\mu_l \Delta T_s L}\right]^{0.25} \tag{4}$$

$$h_{\mathrm{Mod}} = 1.15 h_{\mathrm{Nu}} \tag{5}$$

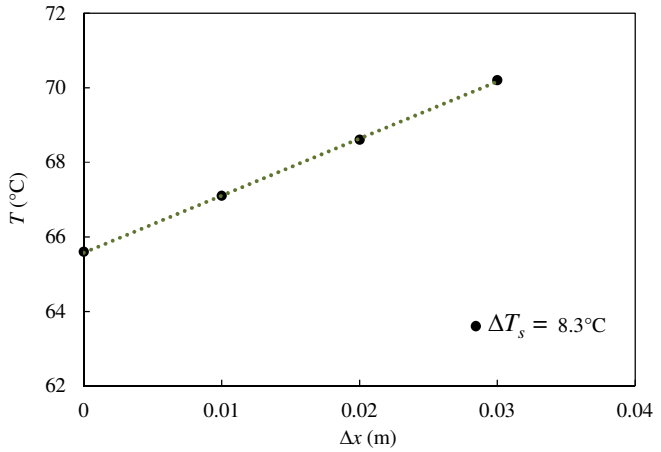

Figure 5 Temperature measurements from thermocouples T_1 to T_4 at $\Delta T_s = 8.3°C$.

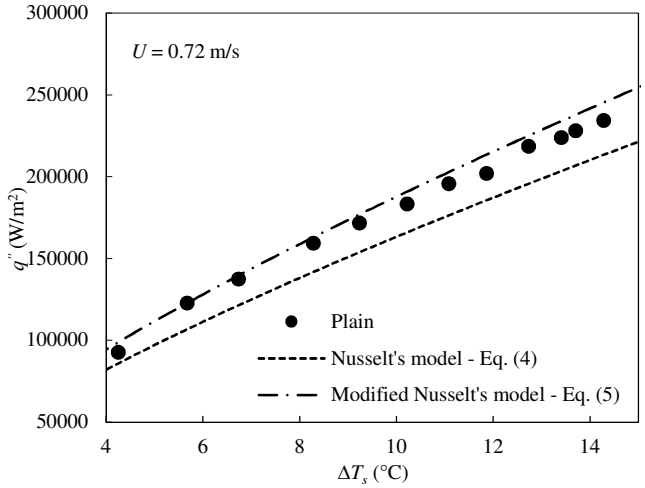

Figure 6 Temperature measurements from thermocouples T_1 to T_4 at $\Delta T_s = 8.3°C$.

Effects of fin spacing

In order to investigate the effects of fin spacing, the micro-fin surfaces were tested at the same vapor velocity of 0.72 m/s and their results are compared against the plain Al-6061 surface. The comparison of the heat flux and heat transfer coefficient at the various wall subcooled temperatures are depicted in Figs. 7 and 8, respectively. It can be seen from these results that the heat transfer performance of the micro-fin surfaces increases with decreasing fin pitch where *MF*3 and *MF*1 exhibit the highest and lowest heat transfer performances, respectively. As shown in Table 1, the reduction in fin pitch corresponds in the increase in fin density hence, resulted in larger total heat transfer area (A_t). However, the experimental results also show that the heat transfer coefficients of the micro-fin surfaces do not increase proportionally with A_t. For instance, even though *MF*1 has 1.56 times larger surface area than the plain Al-6061 surface, the enhancement in h was only about 7% at higher ΔT_s. On the other hand, a more significant increase in h was recorded with *MF*2 and *MF*3 where up to 1.4 times enhancement in h as compared to plain Al-6061 was achieved. Finally, for all the surfaces tested, it can be seen that their h values initially decreased significantly with increasing ΔT_s. However, at higher ΔT_s the rate of reduction in h values decreases, producing exponential decreasing trends as shown in Fig. 8.

As the height of the micro-fins are relatively small (600 μm height), it is possible that a larger portion of the fin flank was flooded by the liquid film resulting in reduced effective fin area for heat transfer. Therefore, micro-fin surface with low fin density (such as *MF*1), may not have sufficient fin surface area which are unflooded for noticeable improvement in heat transfer. On the other hand, when the fin spacing is significantly reduced (such as *MF*3), the high fin density may have impeded the drainage of condensate which increase the liquid film thickness and limits the magnitude of enhancement. In the present investigation, it was determined that the fin spacing of 600 μm (*MF*2) produced the largest rate of increase in enhancement with the reduction in fin pitch.

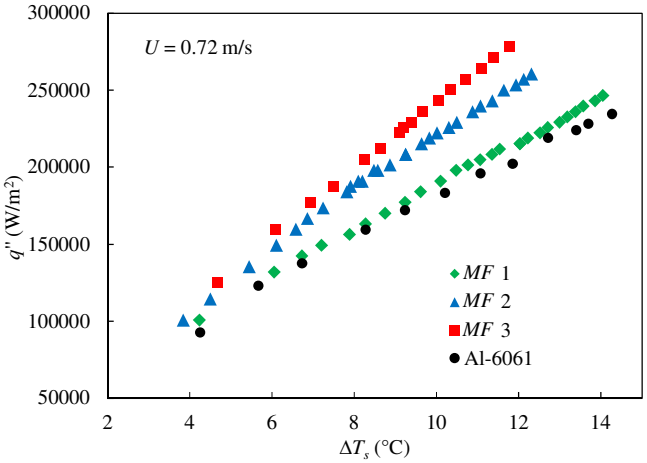

Figure 7 Comparison of q'' vs ΔT_s of plain Al-6061 and micro-fin surfaces at $U = 0.72$ m/s.

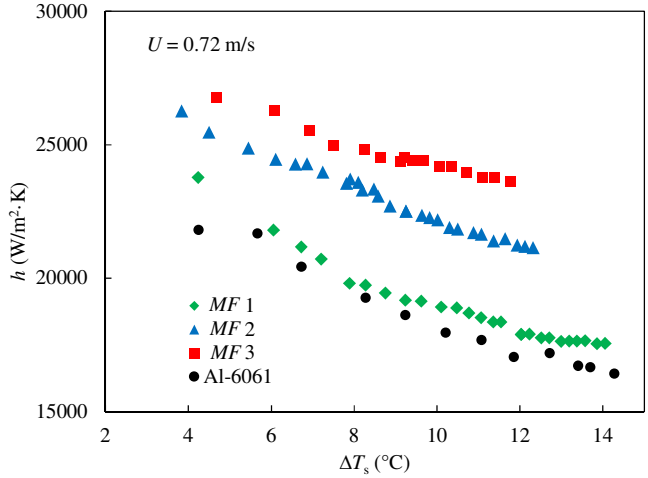

Figure 8 Comparison of h vs ΔT_s of plain Al-6061 and micro-fin surfaces at $U = 0.72$ m/s.

Effects of vapor velocity

The *MF*2 surface was used to investigate the effects of vapor velocity. The surface was tested at the vapor velocities of 0.72 m/s, 1.51 m/s and 2.54 m/s and the results are shown in Figs. 9 and 10. It can be seen from Fig. 9 that at low ΔT_s, vapor velocity (U) has negligible effect on q''. However, with the increment in ΔT_s above 8.5°C, a systematic increase in q'' was observed. Even though the increment in U from 0.72 m/s to 2.54 m/s is not large, a noticeable increase in h was achieved. For instance, at ΔT_s of approximately 12°C, the h values of *MF*2 increased from 21,200 W/m^2·K to 23,200 W/m^2·K as U is increased from 0.72 m/s to 2.45 m/s.

The increase in h values with increasing U has been reported by several researchers [6 - 8]. In the present investigation, even though the vapor shear force and gravitational force on the condensate film are in orthogonal directions, enhancements in h were similarly achieved.

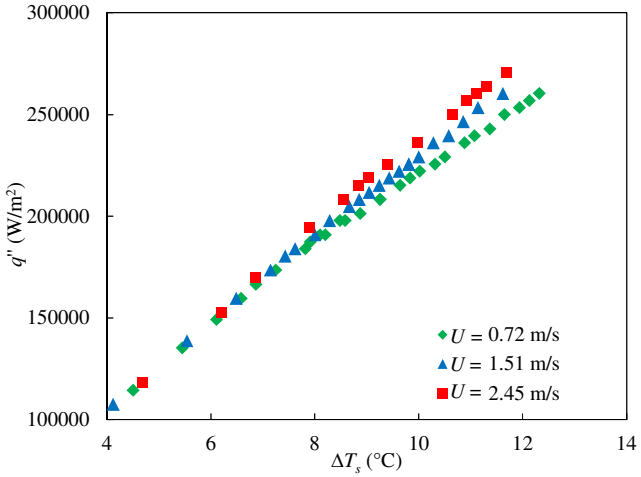

Figure 9 Comparison of q'' vs ΔT_s of *MF*2 at different U.

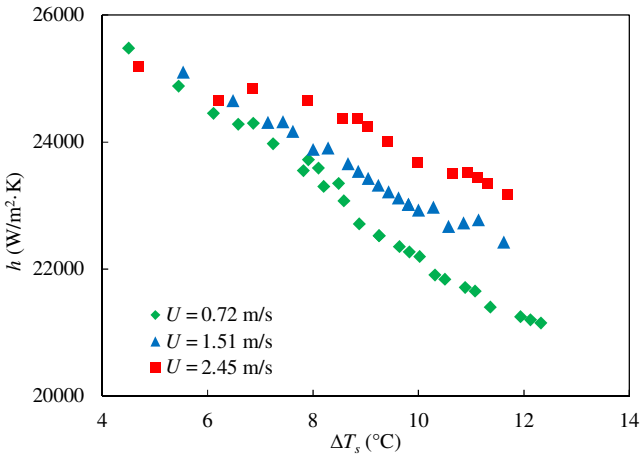

Figure 10 Comparison of h vs ΔT_s of *MF*2 at different U.

CONCLUSION

The effects of fin pitch and vapor velocity on the condensation heat transfer of micro-fin surfaces were experimentally investigated. The results show that *MF*3 with fin pitch of 300 μm demonstrated the highest h values as compared to other micro-fin surfaces whereas *MF*2 with fin pitch of 600 μm demonstrated the largest rate of increase in enhancement with the reduction in fin pitch. The results suggest that for small fin heights, the fin density has to be sufficiently large for noticeable enhancements in h to be achieved. Even though the vapor flow and gravity driven condensate flow are in orthogonal directions, the experimental results with *MF*2 showed that an increase in vapor velocity also resulted in a systematic increase in q'' and h values. In all, up to 1.4 times enhancement was achieved with *MF*3 as compared to the plain Al-6061 surface.

ACKNOWLEDGMENT

Funding for the SLM facility by the National Research Foundation, Singapore, is gratefully acknowledged.

REFERENCES

[1] Del Col, D., Parin, R., Bisetto, A., Bortolin, S., Martucci, A., Film condensation of steam flowing on a hydrophobic surface, *International Journal of Heat and Mass Transfer*, Vol. 107, pp. 307-218 (2017).

[2] Mori, Y., Hijikata, K., Hirasawa, S., Nakayama, W., Optimized performance of condenser with outside condensing surfaces, *Journal of Heat Transfer*, Vol. 103, pp. 96-102 (1981).

[3] Honda, H., Nozu, S., A prediction method for heat transfer during dyring film condensation on horizontal low intergral-fin tubes, *Journal of Heat Transfer*, Vol. 109, pp, 216-225 (1987).

[4] Adamek, T., Webb, R.L., Prediction of film condensation on horizontal integral fin tubes, *International Journal of Heat and Mass Transfer*, Vol., 33, pp. 1721-1735 (1990).

[5] Rose, J.W., An approximate equation for the vapour-side heat-transfer coefficient for condensation on low-finned tubes, *International Journal of Heat and Mass Transfer*, Vol. 37, pp. 865-875 (1994).

[6] Honda, H., Uchima, B., Nozu, S., Torigoe, E., Imai, S., Film condensation of R-113 on staggered bundles of horizontal finned tubes, *Journal of Heat Transfer*, Vol. 114, pp. 443-449 (1992).

[7] Zhang, Z., Li, Q., Xu, T., Fang, Z., Gao, X., Condensation heat transfer characteristics of zeotropic mixture R407C on single, three-row petal-shaped finned tubes and helically baffled condenser, *Applied Thermal Engineering*, Vol. 39, pp. 63-69 (2012).

[8] Fitzgerald, C.L., Briggs, A., Rose, J.W., Wang, H.S., Effect of vapour velocity on condensate retention between fins during condensation on low-finned tubes,

International Journal of Heat and Mass Transfer, Vol. 55, pp. 1412-1418 (2012).

[9] Ali, H.M., Abubaker, M., Effect of circumferential pin thickness on condensate retention as a function of vapor velocity on horizontal pin-fin tubes, *Applied Thermal Engineering*, Vol. 91, pp. 245-251 (2015).

[10] Yau, K.K., Cooper J.R., Rose, J.W., Effect of fin spacing on the performance of horizontal integral-fin condenser tubes, *Journal of Heat Transfer*, Vol. 107, pp. 377-383 (1985).

[11] Ali, H.M., Briggs, A., Condensation of ethylene glycol on pin-fin tubes: effects of circumferential pin spacing and thickness *Applied Thermal Engineering*, Vol. 49, pp. 9-13 (2012).

[12] Nusselt, W., Die Oberflachenkondensation des Wasserdampfes, VDI-Z. 60, pp 541-546 and pp. 569-575 (1916).

[13] Baehr, H.D., Stephan, K., *Heat and Mass Transfer*, 2nd Edition, Springer (2006).

[14] Moffat, R.J., Using uncertainty analysis in the planning of an experiment, *Journal of Fluids Engineering,* Vol. 107, pp. 173-178 (1985).